



ELSEVIER

# Towards neural circuit reconstruction with volume electron microscopy techniques

Kevin L Briggman and Winfried Denk

Electron microscopy is the only currently available technique with a resolution adequate to identify and follow every axon and dendrite in dense neuropil. Reconstructions of large volumes of neural tissue, necessary to reconstruct even local neural circuits, have, however, been inhibited by the daunting task of serially sectioning and reconstructing thousands of sections. Recent technological developments have improved the quality of volume electron microscopy data and automated its acquisition. This opens up the prospect of reconstructing almost complete invertebrate and sizable fractions of vertebrate nervous systems. Such reconstructions of complete neural wiring diagrams could rekindle the tradition of relating neural function to the underlying neuroanatomical circuitry.

## Addresses

Max-Planck Institute for Medical Research, Jahnstrasse 29,69120 Heidelberg, Germany

Corresponding author: Briggman, Kevin L  
(Kevin.Briggman@mpimf-heidelberg.mpg.de)

**Current Opinion in Neurobiology** 2006, **16**:562–570

This review comes from a themed issue on  
New technologies  
Edited by Edward M Callaway and Joshua R Sanes

Available online 8th September 2006

0959-4388/\$ – see front matter

© 2006 Elsevier Ltd. All rights reserved.

DOI [10.1016/j.conb.2006.08.010](https://doi.org/10.1016/j.conb.2006.08.010)

## Introduction

Advances in optical and electrical recording technologies now enable systems neuroscientists to record activity in relatively large populations of neurons with single cell resolution and without averaging across trials [1–5] and then search for activity patterns related to computational processes [6,7]. A key quality to these experiments is the simultaneous recording of many cells, enabling one to take advantage of information contained in co-varying activity. A profound limitation to the interpretation of these datasets is the lack of a detailed wiring diagram relating the observed signals to circuit connectivity. In the absence of anatomical connectivity information, statistical connectivity rules formed on the basis of proximity (e.g. Peters' rule; [8,9]) are used; attempts have also been made to infer 'functional connectivity' from activity correlations in populations [10]. However, knowing the circuit diagram of the actual network from which one has recorded could fundamentally change the way in

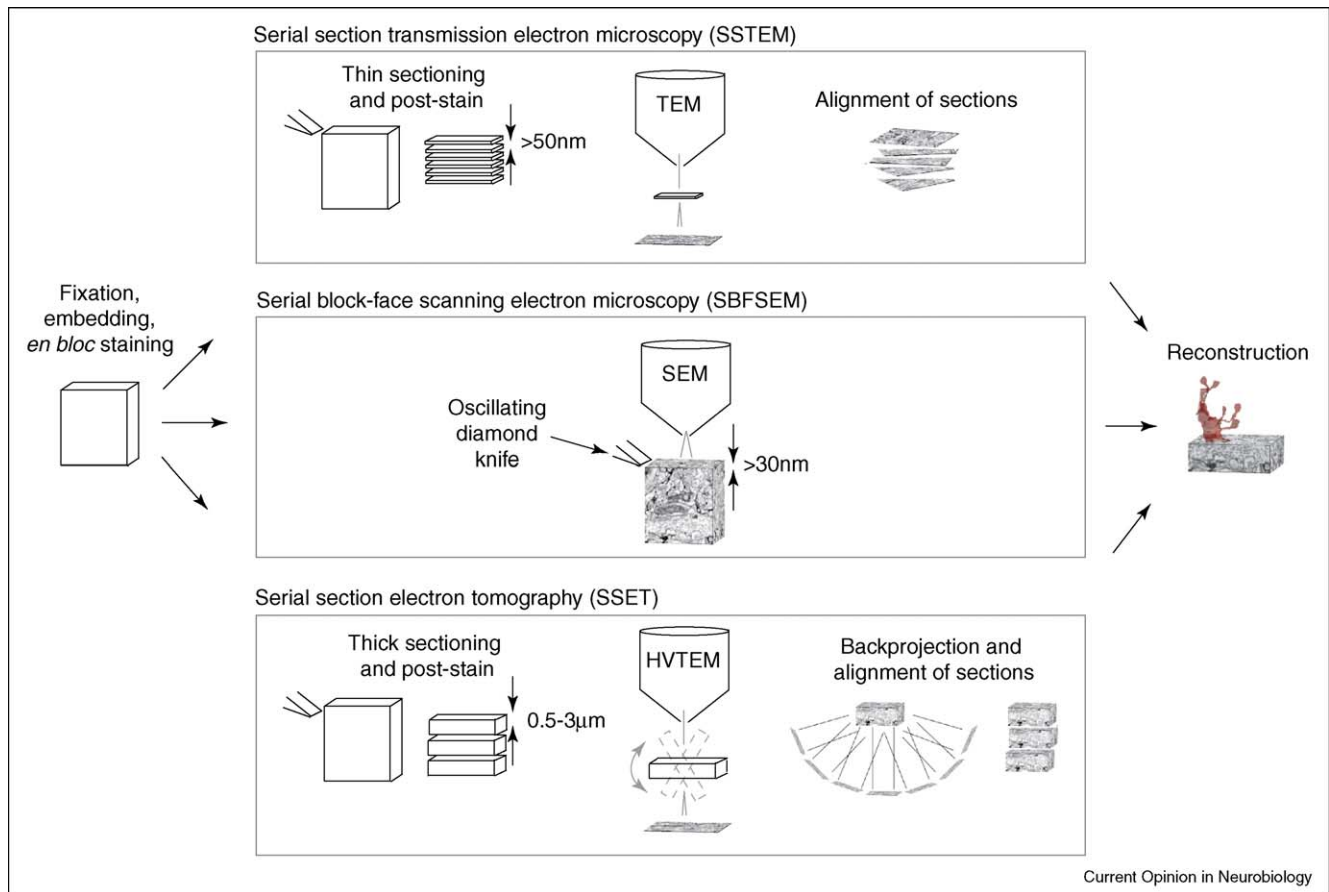
which population data are analyzed and interpreted and might ultimately be necessary to decode neural algorithms.

We learn little about the computations performed by local neural circuits by recording from one neuron at a time, and instead need the ability to cross correlate the activity of multiple — ideally all — neurons involved. Similarly, the knowledge of the morphology of an individual neuron is of limited use to determine circuit connectivity. In other words, the morphology of a single neuron might provide details useful for understanding computations in single cells [11], but knowledge of all the pre- and postsynaptic synaptic connections of a cell is necessary to understand its role in a network. The reconstruction of all neurons in a sufficiently large volume with adequate resolution to identify synaptic connections would constrain models enormously. For both invertebrate and vertebrate nervous systems, it is widely accepted that the connections between neurons are specific, based on neuron type, and not randomly distributed [12–14]. Elucidation of the complete connectivity matrix for a particular piece of tissue might reveal high-order connection statistics and specific patterns of connectivity that are crucial for understanding neural computations. We, therefore, believe that the connectivity matrices representing specific anatomical patterns must be derived from reconstructions of large volumes of neural tissue and not inferred from generalized statistical descriptions of cell and synapse densities.

The techniques available for the reconstruction of large tissue volumes are dictated by the required resolution. Some of the narrowest neuronal processes in the mammalian brain are unmyelinated axons (~100 nm in diameter; [15]) and the thinnest necks of dendritic spines (~50 nm in diameter, [16]). These structures are too small to be resolved by 3D light-microscopy techniques such as confocal [17] or two-photon microscopy [18]; only electron microscopy (EM) has sufficient resolution to reveal them.

In this review, we focus on EM techniques suitable for the reconstruction of neural circuits in their entirety (Figure 1). Traditionally, three dimensional reconstruction of neural tissue has been achieved by serial section transmission electron microscopy (SSTEM) of ultrathin sections [19] (Figure 2). An alternative is serial block-face scanning electron microscopy (SBFSEM; [20]), in which data acquisition is automated and subsequent-section alignment is no longer an issue. We also discuss serial section electron tomography (SSET; [21]).

Figure 1



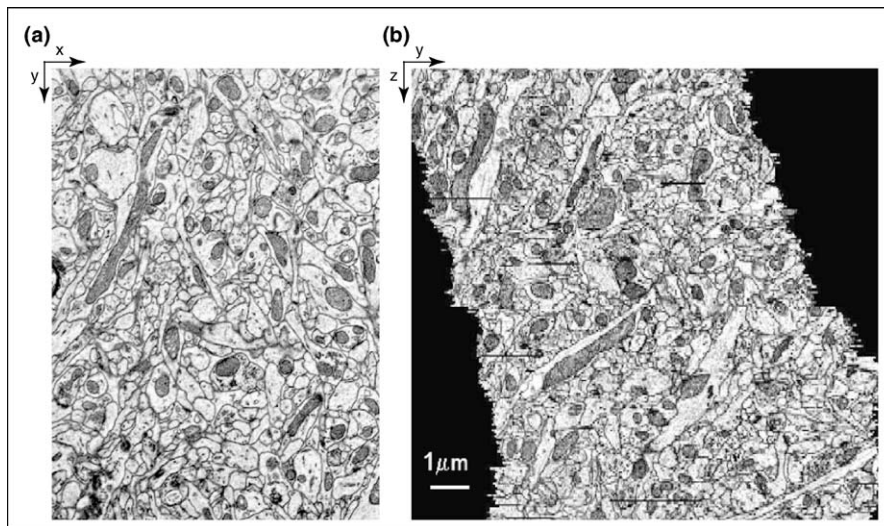
A schematic diagram of the steps involved in the acquisition of tissue volumes using SSTEM, SBFSEM and SSET. The main differences between these techniques are how sections are cut from embedded tissue blocks, the process of image acquisition and the subsequent alignment of images. Sections are cut prior to imaging in SSTEM and SSET, but after imaging in SBFSEM. Transmission electron microscopy (TEM) and high-voltage transmission electron microscopy (HVTEM) are imaging techniques that require 'transparent' samples; scanning electron microscopy (SEM), however, is a surface imaging technique. Image stacks collected in the SBFSEM need no further alignment prior to reconstruction. See text for a more detailed description of each technique.

## Staining

Before discussing imaging techniques *per se*, we need to address the issue of selective staining, which is essential for all reconstruction efforts. Contrast in electron micrographs depends on the accumulation of heavy electron-dense (heavy metal) atoms on the structures of interest. For the purposes of circuit reconstruction, a stain selective for neuron plasma (but not internal) membranes, synaptic vesicles, and post-synaptic densities would be ideal. Standard EM staining protocols rely on various combinations of osmium tetroxide, uranyl acetate, lead citrate and a number of other compounds to stain sub-cellular structures [22], but these techniques are not selective for the plasma membrane. The identification of single neurons within tissue sections historically relied on the Golgi-EM method [23]. Modern techniques enable the intracellular filling of neurons that were first characterized electrophysiologically by injecting

biocytin [24], biotinylated dextran amine (BDA; [25]) or horseradish peroxidase (HRP; [26]). In all cases it is ultimately HRP that catalyses, through the creation of free oxygen radicals from hydrogen peroxide, the oxidation-assisted polymerization of a chromogen, usually diaminobenzidine (DAB; [27]). Subsequent heavy-metal intensification of DAB yields an electron density [28]. DAB polymerization has also been used to 'photo-convert' fluorescent probes into electron-dense products. Photo-conversion of chromophores such as resorufin-based arsenical hairpin binder (ReAsh) [29] thus enables correlation between structures observed in living tissue with the same structures in electron micrographs. Quantum dots of different size and shape can also be discriminated in the transmission electron microscope (TEM), further aiding correlations between light microscopy and EM studies [30]. A complementary approach is to stain the extracellular space, which, in particular with suppressed staining

Figure 2



Serial section transmission electron microscopy. Ultrathin 50 nm sections of rat neocortex imaged with TEM at 7 nm lateral resolution. **(a)** TEM image of a single section (xy plane). **(b)** Registered (aligned) stack of 239 sections resectioned *in silico* (yz plane). Data courtesy of G Knott, registration by DB Chklovskii.

of intracellular organelles, would substantially aid reconstruction. Interstitial staining has been attempted using HRP–DAB (Figure 3a), lanthanum nitrate [31] or transgenic expression of HRP on the cell surface [32].

### Serial section transmission electron microscopy

The well-established technique of SSTEM [33–35] is responsible for the vast majority of studies of neuronal circuitry at EM resolution during the past 30 years. SSTEM is a conceptually simple technique (Figure 1), but the sectioning process is tedious and prone to error. Thick blocks (several hundred  $\mu\text{m}$ ) of tissue are first fixed, usually in some type of aldehyde, and then embedded in a polymeric material, usually a type of epoxy resin. The embedded block is then serially sectioned with a diamond knife on an ultramicrotome, yielding ribbons of thin sections. Staining can be performed *en bloc* or, after sectioning, on the thin sections. It was recently demonstrated that both neuronal ultrastructure and immunoreactivity in thin sections is better preserved through the process of high-pressure freezing than by conventional fixation [36,37].

Ribbons of sections are transferred onto grids for imaging with TEM. In the TEM image, contrast is due mainly to the increased elastic scattering of electrons in areas containing the heavy metal stain as they travel through a thin section [38]. The sectioning and transfer processes are susceptible to many problems—even for experienced practitioners—including loss of sections, uneven section thickness, debris on sections and geometrical distortion. Even if the sections can be successfully imaged,

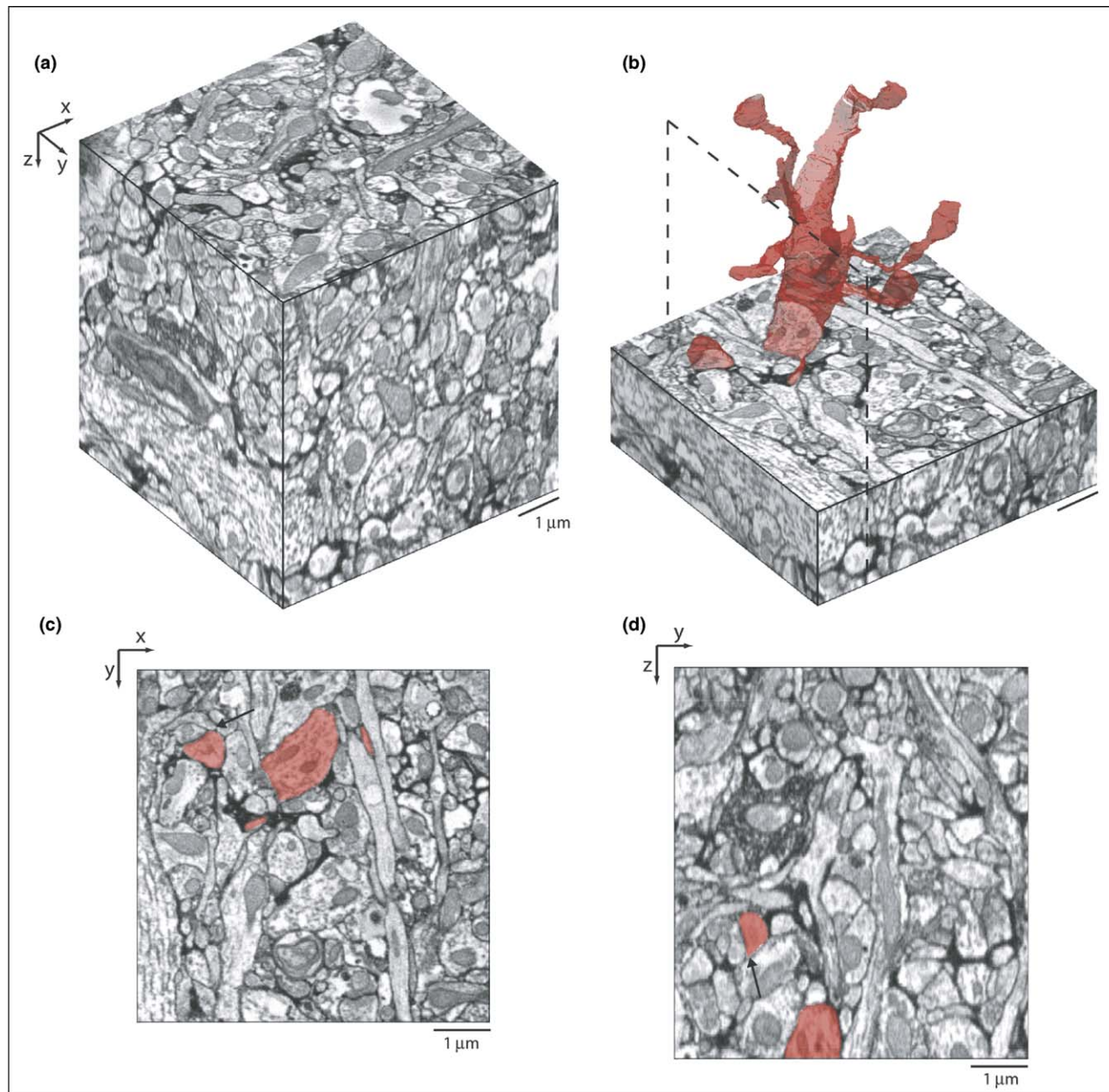
distortions, which vary locally and between sections, hamper automated approaches for the alignment and reconstruction of fine neuronal processes (but see Figure 2).

In TEM, the lateral resolution of ultra-thin sections can be better than 10 nm, depending somewhat on the type of stain employed. Although high-energy electrons can penetrate sections as thick as 10  $\mu\text{m}$  [39], albeit at some loss of resolution, merely projections rather than three-dimensionally resolved data are obtained, because of the large depth of field of electron microscopes. Ultra-thin sections are, therefore, used to generate resolution perpendicular to the sectioning plane. Thick sections can, however, be virtually sectioned using electron tomography (discussed below). Although section thicknesses as thin as 25 nm have been claimed [35], most studies have not been able to achieve long series of sections thinner than 50 nm, partly because of poor formation of section ribbons (JG White, pers comm). A resolution of 50 nm along the depth (Z) axis does not enable the reliable reconstruction of, for example, thin dendritic spine necks. The difference between the lateral and the depth resolutions is apparent when comparing xy and xz images in Figure 2.

Although SSTEM has successfully been used to reconstruct small lengths of dendrites [16] and axons [15], we focus here on attempts to reconstruct neuronal circuitry, which, in most cases, requires reconstructing dendritic arborizations in their entirety. The largest such reconstruction performed to date is that of the entire nervous system of the nematode *Caenorhabditis elegans* [40]. This



Figure 3



Serial block-face scanning electron microscopy. **(a)** A  $350 \mu\text{m}^3$  volume from adult rat barrel cortex sampled at  $13.2\text{nm}/\text{pixel}$  in the  $xy$  plane consisting of 253 sections  $30 \text{ nm}$  thick. **(b)** Manually traced spiny dendrite. The dotted line indicates the location of the slice shown in panel d. **(c)** A sample  $xy$  plane. The arrow points to a spine head and a synaptic density. **(d)** A sample  $yz$  plane. The arrow points to the same structure as in (c). Unpublished data of KL Briggman, RM Bruno, W Denk, T Euler and H Horstmann.

seminal study identified the morphologies of all 302 neurons and their 5000 chemical synaptic connections using approximately 8000 serial sections of  $50 \text{ nm}$  section thickness. This achievement has profoundly influenced subsequent studies of the function of neural circuits in this species. One example is the neural circuit for touch sensitivity, the anatomy, function and development of

which was elucidated by using the circuit diagram to first guide single-cell laser ablation studies and then to interpret their results [41].

SSTEM has also been applied to the study of retinal circuitry [42] and to the mammalian hippocampus [43] and cortex [44]. Partial reconstructions of major cell

classes in the vertebrate retina have helped to reveal distributions of synapses along dendrites and the identity of pre- and post-synaptic partners (e.g. [35,45–47]). However, insufficient Z-axis resolution made tracing the axons of some bipolar cells impossible because of their “extremely fine and tortuous” nature [46]. Importantly, SSTEM studies of the retina demonstrated that the complexity of circuit connectivity exceeds what had previously been suspected [48]. Reconstructions of synapses along lengths of dendrites and axons (ranging from 10–100  $\mu\text{m}$ ) have also been obtained from the visual [49,50] and somatosensory [51] areas of the cortex. A major thrust of these studies has been to search for patterns of synaptic input into layer 4 spiny stellate neurons [52].

A cursory search in the primary literature on the use of SSTEM for the purpose of neuronal circuit reconstruction reveals a rapid decrease in the number of published studies towards the end of the 1980s. This perhaps coincides with the introduction of high-resolution optical sectioning techniques [53] and genetically targeted fluorescence tracer molecules [54]. Such techniques offer a clear advantage in time and effort to identify connections between stained pairs of neurons. However, although super-resolution techniques [55,56] might be able to do so in the future, current optical methods are not capable of resolving axon and dendrite trajectories or unambiguously identifying synaptic contacts among thousands of neurons in a dense neuropil. For example, assuming that single synapses occur only at axon varicosities might overlook whole classes of subcircuits [57].

With the exception of the *C. elegans* reconstruction ( $\sim 10^6 \mu\text{m}^3$ ; [58]), in which only neurons have been traced and which constitute only a small fraction of the body volume, the volumes of neural tissue that have been reconstructed from individual specimens are in the order of  $10^3 \mu\text{m}^3$ . These volumes are far smaller than, for example, the volume necessary to reconstruct a complete *Drosophila* brain ( $\sim 10^8 \mu\text{m}^3$ ; [58]) or a single cortical column from a mouse ( $\sim 10^8 \mu\text{m}^3$ ; [59]). Given that the *C. elegans* reconstruction took about 15 years to complete (JG White, pers commun), manual SSTEM reconstructions of such large volumes appears impractical.

### Serial block-face scanning electron microscopy

The SBFSEM automates the process of sectioning and imaging blocks of tissue by incorporating a custom microtome into a low-vacuum SEM chamber [20,60,61]. Unlike a TEM, the images in an SEM are generated from electrons scattered off the surface of an embedded tissue sample, making the imaging of block faces possible [62]. Existing *en bloc* stains, such as uranyl acetate and osmium, provide adequate contrast, and a lateral resolution of better than 30 nm is possible [20]. Sections are cut from

the surface of the block with an oscillating diamond knife. It is possible to cut series of hundreds if not thousands of sequential sections [20] with a section thickness of as little as 30 nm (KL Briggman, W Denk, unpublished, Figure 3).

There are several crucial advantages of SBFSEM over traditional SSTEM. Because the images are taken directly from the block face prior to each cut, the problems of sections being distorted or lost during handling are completely avoided. Furthermore, the images in raw SBFSEM datasets are already aligned and are, therefore, amenable to fully automated analysis techniques. Because the sectioning process is fully automated, large volumes can be imaged without significant operator involvement.

In most cases the area to be imaged is many times larger than the field of view of the SEM at the required resolution; it is, therefore, necessary to take multiple images to cover block faces as large as 500  $\mu\text{m}$ . The microtome, therefore, needs to be mounted on a translation stage with a mechanical reproducibility better than the lateral resolution (10 nm) in order to maintain the alignment within and between subimage stacks.

The SBFSEM has been used to section successfully small volumes of cortex, cerebellum, retina, zebrafish brain, and fly brain. Examples of such datasets are available online [20]. The quality of recent datasets enables single retinal processes to be followed manually through image stacks  $>100 \mu\text{m}$  along the Z-axis. Current efforts are underway to further reduce the section thickness below 30 nm and to improve intra- versus extra-cellular staining contrast.

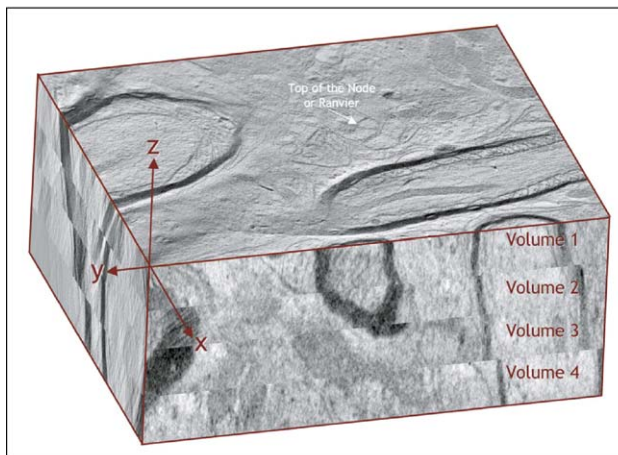
The speed of SBFSEM is ultimately limited by the pixel dwell time necessary to achieve a reasonable signal-to-noise ratio, with rates of slightly above 100 kHz currently being used (KL Briggman, W Denk, *et al.* unpublished, see also Figure 3). At this rate the time needed to collect  $10^7 \mu\text{m}^3$  (at 30 nm<sup>3</sup> resolution) would be about a month.

### Serial section electron tomography

One alternative to SSTEM is SSET [21], which is based on the principle of reconstructing a 3D structure from multiple 2D projections at varying angles, a method similar to computed tomography (CT) scans in medical radiology [37,63,64]. The 3D structure can be reconstructed from the 2D tilt-series of images by a variety of back projection techniques [65]. SSET reduces the number of sections that need to be cut for a given total sample thickness and also improves the Z-axis resolution below that of the thinnest sections that can currently be cut by a microtome. SSET has been used to reconstruct a number of subcellular structures, including dendritic spines [66] and nodes of Ranvier [67\*] (see Figure 4).

Blocks of tissue are stained and embedded, similar to the process in SSTEM, and then sectioned into thick

Figure 4



Serial section tomographic reconstruction of a CNS node of Ranvier. This reconstruction contains 90–95% of the entire width of the node of Ranvier and includes the axon, myelin layers and astrocytic processes (for details see [67\*]). Each thick section was  $\sim 1.5 \mu\text{m}$  thick. The faces of this cube represent orthogonal xy, yz, and xz slices of the reconstruction. Data courtesy of GE Sosinsky and MH Ellisman.

(0.5–3  $\mu\text{m}$ ) sections. Note that in SSET (as in SBFSEM) post-section staining methods (such as post-embedding immuno-staining) cannot be used. Tilt series are obtained by imaging a section at 1–2° increments in a high-voltage TEM (HVTEM). The specimen is ideally tilted along both the X- and the Y- axes through angles as large as  $\pm 70^\circ$ , which optimizes Z-axis resolution and reduces the range of missing spatial frequencies (missing wedge and pyramid), which are responsible for reconstruction artifacts. Because at such extreme angles the effective electron path length is almost three times the section thickness, energy filtering techniques are essential for thicker sections to reach resolutions of better than 10 nm along all dimensions [68,69].

The appeal of SSET is a large reduction in the number of sections that need to be cut for an equivalent volume compared with the number needed for either SSTEM or SBFSEM, reducing the risk of section damage and loss. Although for some applications the loss of material between sequential thick sections, estimated to be 15–25 nm in a SSET reconstruction of the Golgi complex in rat kidney cells [70] is a concern, it might not seriously affect the ability to reconstruct neural processes. However, distortion and shrinkage of tissue caused by the large electron dose needed for the acquisition of a full tilt-series, which comprises as many as 150 images [71], needs to be detected and corrected.

## Reconstruction

As computer processing power and storage capacity have increased, efforts have been made to automate the

tedious task of manually tracing neuronal processes through dense neuropil. One of the earliest uses of computer-assisted tracing was a reconstruction of a portion of the optic ganglion in the small crustacean *Daphnia magna* [72,73]. There is now a plethora of freely or commercially available semi-automated reconstruction software packages providing morphometric operations, region growing techniques, and interfaces for digitizing tablets (e.g., [74–76]). Given the estimate that computer-assisted tracings by humans can be performed at a rate of  $\sim 1 \mu\text{m}^3/\text{hour}$  [58], a manual reconstruction of a mouse cortical column would take  $>10\,000$  person years. Indeed, the most time-consuming step in the *C. elegans* reconstruction was the manual tracing and tracking of neuronal processes (JG White, pers commun). Thus, for even modestly large volumes, the amount of user interaction per volume to be traced needs to be rather small and reconstructions will need to be almost fully automated, perhaps involving the development of new machine-learning algorithms [77–79]. The complexity of this task can be appreciated, for example, by viewing the available SBFSEM datasets [20]. Automated reconstruction will greatly benefit from staining protocols that clearly distinguish between the neuronal plasma membranes (or the extracellular space) and the intracellular membranes.

## Correlating structure with function

In almost all areas of biology the need to find the detailed connection between biochemical function, such as synaptic vesicle fusion, and (macromolecular) structure is undisputed. (A, by now, classical example being the electron tomographic reconstructions of the neuromuscular synapse [80].) In systems neurobiology, the utility of having structural (connectivity) information is undisputed as well, and was the main motivation behind the complete reconstruction of the *C. elegans* nervous system, which has demonstrated how knowledge of the circuitry can be combined with selective ablations and genetic manipulations [41,81,82]. The need for having the complete connectivity map for a particular instantiation of the nervous system in order to discover and understand the neural algorithms is more in dispute, possibly partly out of desperation in the face of the enormity of the task [83]. For more complex nervous systems, such as a single mouse cortical column or a complete mouse brain, the number of neurons will be  $10^4$  and  $10^7$  times larger; the number of synaptic connections will be  $10^7$  and  $10^{11}$  times larger; and the volumes will be  $10^2$  and  $10^5$  times larger, respectively [9,58,84]. One advantage that mammals, in particular, have over the nematode is the availability of physiological data acquired by both electrical [1,85] and optical [2–4] means.

Although the reconstruction of even a single cortical column appears daunting, it appears just feasible. Initial experiments (KL Briggman, RM Bruno, W Denk, *et al.*, unpublished) show that thousands of multi-tiled slices (each more than  $10^8$  pixels) can be acquired using the



SBFSEM technology within a matter of months. In particular, the prospect of combining physiological population recordings with a post-hoc determination of the underlying neuronal circuitry studies might turn out to be the missing link in finding neural algorithms. At the very least, such detailed knowledge will enable us to validate hypotheses about the geometrical statistics of neural wiring [86\*\*].

## Conclusions

Detailed neuroanatomy could well be in for a serious comeback as the technology needed to reconstruct entire local circuits, and perhaps (for *Drosophila*) entire brains, at the resolution needed to follow each and every neural 'wire' is becoming available at the level of both data acquisition and data analysis. Although the interpretation of the data (in the form of, say, a matrix with 10 000 rows and 10 000 columns and synaptic weights as the 10<sup>8</sup> matrix elements) will be another challenge, every theory of how any neural computation works will have to be consistent with the measured connectivity.

## Acknowledgments

We thank DB Chklovskii and JG White for helpful discussions and comments on this manuscript. We also thank G Knott, DB Chklovskii, MH Ellisman, and GE Sosinsky for figure contributions.

## References and recommended reading

Papers of particular interest, published within the annual period of review, have been highlighted as:

- of special interest
- of outstanding interest

1. Buzsaki G: **Large-scale recording of neuronal ensembles.** *Nat Neurosci* 2004, **7**:446-451.
  2. Ikegaya Y, Le Bon-Jego M, Yuste R: **Large-scale imaging of cortical network activity with calcium indicators.** *Neurosci Res* 2005, **52**:132-138.
  3. Ohki K, Chung S, Ch'ng YH, Kara P, Reid RC: **Functional imaging with cellular resolution reveals precise micro-architecture in visual cortex.** *Nature* 2005, **433**:597-603.
  4. Kerr JN, Greenberg D, Helmchen F: **Imaging input and output of neocortical networks in vivo.** *Proc Natl Acad Sci USA* 2005, **102**:14063-14068.
  5. Yaksi E, Friedrich RW: **Reconstruction of firing rate changes across neuronal populations by temporally deconvolved Ca2+ imaging.** *Nat Methods* 2006, **3**:377-383.
  6. Dragoi G, Buzsaki G: **Temporal encoding of place sequences by hippocampal cell assemblies.** *Neuron* 2006, **50**:145-157.
  7. Friedrich RW, Habermann CJ, Laurent G: **Multiplexing using synchrony in the zebrafish olfactory bulb.** *Nat Neurosci* 2004, **7**:862-871.
  8. Peters A: **Thalamic input to the cerebral cortex.** *Trends Neurosci* 1979, **2**:183-185.
  9. Braitenberg V, Schüz A: *Cortex: Statistics and Geometry of Neuronal Connectivity*, edn 2. Springer; 1998.
  10. Okatan M, Wilson MA, Brown EN: **Analyzing functional connectivity using a network likelihood model of ensemble neural spiking activity.** *Neural Comput* 2005, **17**:1927-1961.
  11. London M, Häusser M: **Dendritic computation.** *Annu Rev Neurosci* 2005, **28**:503-532.
  12. White EL: **Specificity of cortical synaptic connectivity: emphasis on perspectives gained from quantitative electron microscopy.** *J Neurocytol* 2002, **31**:195-202.
  13. Song S, Sjöström PJ, Reigl M, Nelson S, Chklovskii DB: **Highly nonrandom features of synaptic connectivity in local cortical circuits.** *Plos Biol* 2005, **3**:507-519.
  14. Yoshimura Y, Callaway EM: **Fine-scale specificity of cortical networks depends on inhibitory cell type and connectivity.** *Nature Neuroscience* 2005, **8**:1552-1559.
  15. Shepherd GMG, Harris KM: **Three-dimensional structure and composition of CA3 -> CA1 axons in rat hippocampal slices: Implications for presynaptic connectivity and compartmentalization.** *J Neurosci* 1998, **18**:8300-8310.
  16. Fiala JC, Harris KM: **Dendrite structure.** In *Dendrites*. Edited by Stuart G, Spruston N, Häusser M. Oxford University Press; 1999.
  17. Conchello JA, Lichtman JW: **Optical sectioning microscopy.** *Nat Methods* 2005, **2**:920-931.
  18. Denk W, Strickler JH, Webb WW: **2-photon laser scanning fluorescence microscopy.** *Science* 1990, **248**:73-76.
  19. Ware RW: **Three-dimensional reconstruction from serial sections.** *Int Rev Cytol* 1975, **40**:325-440.
  20. Denk W, Horstmann H: **Serial block-face scanning electron microscopy to reconstruct three-dimensional tissue nanostructure.** *Plos Biol* 2004, **2**:1900-1909.
  21. Soto GE, Young SJ, Martone ME, Deerinck TJ, Lamont S, Carragher BO, Hama K, Ellisman MH: **Serial section electron tomography: a method for three-dimensional reconstruction of large structures.** *Neuroimage* 1994, **1**:230-243.
  22. Hayat MA: *Principles and Techniques of Electron Microscopy: Biological Applications*, edn 4. Cambridge University Press; 2000.
  23. Fairen A: **Pioneering a golden age of cerebral microcircuits: the births of the combined Golgi-electron microscope methods.** *Neuroscience* 2005, **136**:607-614.
- A historical account of the development and evolution of the Golgi method for use in EM neuroanatomy.
24. Xue HG, Yang CY, Ito H: **The anterograde and retrograde axonal transport of biotinylated dextran amine and biocytin in the nervous system of teleosts.** *Brain Res Protoc* 2004, **13**:106-114.
  25. Reiner A, Veenman CL, Medina L, Jiao Y, Del Mar N, Honig MG: **Pathway tracing using biotinylated dextran amines.** *J Neurosci Methods* 2000, **103**:23-37.
  26. LaVail JH, LaVail MM: **Retrograde axonal transport in the central nervous system.** *Science* 1972, **176**:1416-1417.
  27. Graham RC Jr, Karnovsky MJ: **The early stages of absorption of injected horseradish peroxidase in the proximal tubules of mouse kidney: ultrastructural cytochemistry by a new technique.** *J Histochem Cytochem* 1966, **14**:291-302.
  28. Adams JC: **Heavy metal intensification of DAB-based HRP reaction product.** *J Histochem Cytochem* 1981, **29**:775.
  29. Gaietta G, Deerinck TJ, Adams SR, Bouwer J, Tour O, Laird DW, Sosinsky GE, Tsien RY, Ellisman MH: **Multicolor and electron microscopic imaging of connexin trafficking.** *Science* 2002, **296**:503-507.
  30. Giepmans BNG, Deerinck TJ, Smarr BL, Jones YZ, Ellisman MH: **Correlated light and electron microscopic imaging of multiple endogenous proteins using Quantum dots.** *Nat Methods* 2005, **2**:743-749.
- This study describes the state of the art in immuno-labeling light microscopy and EM correlation studies. The authors used quantum dot conjugated antibodies to label structures and achieved penetration depths of several microns.
31. Shaklai M, Tavassoli M: **A modified technique to obtain uniform precipitation of lanthanum tracer in the extracellular space.** *J Histochem Cytochem* 1977, **25**:1013-1015.

32. Larsen CW, Hirst E, Alexandre C, Vincent JP: **Segment boundary formation in *Drosophila* embryos.** *Development* 2003, **130**:5625-5635.
33. Macagno ER, Levinthal C, Sobel I: **Three-dimensional computer reconstruction of neurons and neuronal assemblies.** *Annu Rev Biophys Bioeng* 1979, **8**:323-351.
34. Stevens JK, Davis TL, Friedman N, Sterling P: **A systematic approach to reconstructing microcircuitry by electron microscopy of serial sections.** *Brain Res* 1980, **2**:265-293.
35. Sjostrand FS: **Ultrastructure of retinal rod synapses of the guinea pig eye as revealed by 3-dimensional reconstructions from serial sections.** *J Ultrastruct Res* 1958, **2**:122-170.
36. Rostaing P, Weimer RM, Jorgensen EM, Triller A, Bessereau JL: **Preservation of immunoreactivity and fine structure of adult *C. elegans* tissues using high-pressure freezing.** *J of Histochem Cytochem* 2004, **52**:1-12.
37. Leapman RD: **Novel techniques in electron microscopy.** *Curr Opin Neurobiol* 2004, **14**:591-598.
38. Reimer L: *Transmission Electron Microscopy: Physics of Image Formation and Microanalysis*, edn 2. Springer-Verlag; 1989.
39. Glaupert AM: **High voltage electron-microscope in biology.** *J Cell Biol* 1974, **63**:717-748.
40. White JG, Southgate E, Thomson JN, Brenner S: **The structure of the nervous-system of the nematode *Caenorhabditis-Elegans*.** *Philos Trans R Soc Lond B Biol Sci* 1986, **314**:1-340.
41. Chalfie M, Sulston JE, White JG, Southgate E, Thomson JN, Brenner S: **The neural circuit for touch sensitivity in *Caenorhabditis elegans*.** *J Neurosci* 1985, **5**:956-964.
42. Sterling P: **Microcircuitry of the cat retina.** *Annu Rev Neurosci* 1983, **6**:149-185.
43. Sorra KE, Harris KM: **Occurrence and three-dimensional structure of multiple synapses between individual radiatum axons and their target pyramidal cells in hippocampal area CA1.** *J Neurosci* 1993, **13**:3736-3748.
44. White EL, Keller A: *Cortical Circuits: Synaptic Organization of the Cerebral Cortex – Structure, Function, and Theory.* Birkhäuser; 1989.
45. Kolb H, Jones J: **Synaptic organization of the outer plexiform layer of the turtle retina: an electron microscope study of serial sections.** *J Neurocytol* 1984, **13**:567-591.
46. Freed MA, Sterling P: **The on-alpha ganglion-cell of the cat retina and its presynaptic cell-types.** *J Neurosci* 1988, **8**:2303-2320.
47. Famiglietti EV: **Synaptic organization of starburst amacrine cells in rabbit retina - analysis of serial thin-sections by electron-microscopy and graphic reconstruction.** *J Comp Neurol* 1991, **309**:40-70.
48. Mcguire BA, Stevens JK, Sterling P: **Microcircuitry of bipolar cells in cat retina.** *J Neurosci* 1984, **4**:2920-2938.
49. Somogyi P: **The study of Golgi stained cells and of experimental degeneration under the electron microscope: a direct method for the identification in the visual cortex of three successive links in a neuron chain.** *Neurosci* 1978, **3**:167-180.
50. Davis TL, Sterling P: **Microcircuitry of cat visual cortex: classification of neurons in layer IV of area 17, and identification of the patterns of lateral geniculate input.** *J Comp Neurol* 1979, **188**:599-627.
51. Porter LL, White EL: **Synaptic connections of callosal projection neurons in the vibrissal region of mouse primary motor cortex - an electron-microscopic horseradish-peroxidase study.** *J Comp Neurol* 1986, **248**:573-587.
52. Mcguire BA, Hornung JP, Gilbert CD, Wiesel TN: **patterns of synaptic input to layer-4 of cat striate cortex.** *J Neurosci* 1984, **4**:3021-3033.
53. Amos WB, White JG: **How the confocal laser scanning microscope entered biological research.** *Biol Cell* 2003, **95**:335-342.
54. Chalfie M, Tu Y, Euskirchen G, Ward WW, Prasher DC: **green fluorescent protein as a marker for gene-expression.** *Science* 1994, **263**:802-805.
55. Hell SW, Dyba M, Jakobs S: **Concepts for nanoscale resolution in fluorescence microscopy.** *Curr Opin Neurobiol* 2004, **14**:599-609.
56. Betzig E, Patterson GH, Sougrat R, Lindwasser OW, Olenych S, Bonifacino JS, Davidson MW, Lippincott-Schwartz J, Hess HF: **Imaging intracellular fluorescent proteins at nanometer resolution** *Science* 2006, Published online. DOI:10.1126/science.1127344.
57. White EL, Weinfeld E, Lev DL: **Quantitative analysis of synaptic distribution along thalamocortical axons in adult mouse barrels.** *J Comp Neurol* 2004, **479**:56-69.
58. Fiala JC, **Three-dimensional structure of synapses in the brain and on the web.** In *Proceedings of the 2002 International Joint Conference on Neural Networks, May 12–17, Honolulu, Hawaii, 2002*:1–4.
59. McCasland JS, Woolsey TA: **High-resolution 2-deoxyglucose mapping of functional cortical columns in mouse barrel cortex.** *J Comp Neurol* 1988, **278**:555-569.
60. Leighton SB: **Sem images of block faces, cut by a miniature microtome within the Sem – a technical note.** *Scanning Electron Microscopy* 1981:73-76.
61. Kuzirian AM, Leighton SB: **Oxygen plasma-etching of entire block faces improves the resolution and usefulness of serial scanning electron-microscopic images.** *Scanning Electron Microscopy* 1983:1877-1885.
62. Goldstein J: *Scanning Electron Microscopy and X-Ray Microanalysis*, edn 3. Kluwer Academic/Plenum Publishers; 2003.
63. McEwen BF, Marko M: **The emergence of electron tomography as an important tool for investigating cellular ultrastructure.** *J Histochem Cytochem* 2001, **49**:553-563.
64. Frey TG, Perkins GA, Ellisman MH: **Electron tomography of membrane-bound cellular organelles.** *Annu Rev Biophys Biomol Struct* 2006, **35**:199-224.
65. Lawrence A, Bouwer JC, Perkins G, Ellisman MH: **Transform-based backprojection for volume reconstruction of large format electron microscope tilt series.** *J Struct Biol* 2006, **154**:144-167.
66. Shoop RD, Esquenazi E, Yamada N, Ellisman MH, Berg DK: **Ultrastructure of a somatic spine mat for nicotinic signaling in neurons.** *J Neurosci* 2002, **22**:748-756.
67. Sosinsky GE, Deerinck TJ, Greco R, Buitenhuys CH, Bartol TM, Ellisman MH: **Development of a model for microphysiological simulations: small nodes of ranvier from peripheral nerves of mice reconstructed by electron tomography.** *Neuroinformatics* 2005, **3**:133-162.
- The authors reconstructed a node of Ranvier from three 500 nm sections using SSET. The Z-axis resolution of this technique was better than 10 nm, a Z-axis resolution not currently achievable by either SSTEM or SBFSEM.
68. Bouwer JC, Mackey MR, Lawrence A, Deerinck TJ, Jones YZ, Terada M, Martone ME, Peltier S, Ellisman MH: **Automated most-probable loss tomography of thick selectively stained biological specimens with quantitative measurement of resolution improvement.** *J Struct Biol* 2004, **148**:297-306.
69. McIntosh R, Nicastro D, Mastronarde D: **New views of cells in 3D: an introduction to electron tomography.** *Trends Cell Biol* 2005, **15**:43-51.
70. Ladinsky MS, Mastronarde DN, McIntosh JR, Howell KE, Staehelin LA: **Golgi structure in three dimensions: functional insights from the normal rat kidney cell.** *J Cell Biol* 1999, **144**:1135-1149.



71. Martone ME, Deerinck TJ, Yamada N, Bushong E, Ellisman MH: **Correlated 3D light and electron microscopy: Use of high voltage electron microscopy and electron tomography for imaging large biological structures.** *J Histotechnology* 2000, **23**:261-270.
72. Levinthal C, Ware R: **Three dimensional reconstruction from serial sections.** *Nature* 1972, **1972**:207-210.
73. Macagno ER, Lopresti V, Levinthal C: **Structure and development of neuronal connections in isogenic organisms: variations and similarities in the optic system of *Daphnia magna*.** *Proc Natl Acad Sci USA* 1973, **70**:57-61.
74. Perkins GA, Renken CW, Song JY, Frey TG, Young SJ, Lamont S, Martone ME, Lindsey S, Ellisman MH: **Electron tomography of large, multicomponent biological structures.** *J Struct Biol* 1997, **120**:219-227.
75. Fiala JC: **Reconstruct: a free editor for serial section microscopy.** *J Microsc Oxford* 2005, **218**:52-61.
76. Kremer JR, Mastronarde DN, McIntosh JR: **Computer visualization of three-dimensional image data using IMOD.** *J Struct Biol* 1996, **116**:71-76.
77. Bishop CM: *Neural Networks for Pattern Recognition.* Oxford University Press; 1995.
78. Duda RO, Hart PE, Stork DG: *Pattern Classification*, edn 2. Wiley; 2001.
79. Bonnet N: **Some trends in microscope image processing.** *Micron* 2004, **35**:635-653.
80. Harlow ML, Ress D, Stoschek A, Marshall RM, McMahan UJ: **The architecture of active zone material at the frog's neuromuscular junction.** *Nature* 2001, **409**:479-484.
81. Gray JM, Hill JJ, Bargmann CI: **A circuit for navigation in *Caenorhabditis elegans*.** *Proc Natl Acad Sci USA* 2005, **102**:3184-3191.
82. Schafer WR: **Deciphering the neural and molecular mechanisms of *C-elegans* behavior.** *Curr Biol* 2005, **15**:R723-R729.
83. Martin KA: **Microcircuits in visual cortex.** *Curr Opin Neurobiol* 2002, **12**:418-425.
84. Armstrong JD, Kaiser K, Muller A, Fischbach KF, Merchant N, Strausfeld NJ: **Flybrain, an on-line atlas and database of the *Drosophila* nervous system.** *Neuron* 1995, **15**:17-20.
85. Feldmeyer D, Roth A, Sakmann B: **Monosynaptic connections between pairs of spiny stellate cells in layer 4 and pyramidal cells in layer 5A indicate that lemniscal and paralemniscal afferent pathways converge in the infragranular somatosensory cortex.** *J Neurosci* 2005, **25**:3423-3431.
86. Chen BL, Hall DH, Chklovskii DB: **Wiring optimization can relate neuronal structure and function.** *Proc Natl Acad Sci USA* 2006, **103**:4723-4728.

This paper finalizes the *C. elegans* wiring diagram. In addition, it uses the wiring diagram to test theories that the anatomy of neuronal networks is designed to minimize a metric of 'wiring cost'. Studies such as this are not possible without large reconstructions of circuits.